

Studying the Production of a Singlet Scalar at Future e^+e^- Colliders with Deep Neural Networks

Anza-Tshilidzi Mulaudzi^a, Mukesh Kumar^a, Bruce Mellado^{a,b} and Abhaya Kumar Swain^a

^aSchool of Physics and Institute for Collider Particle Physics, University of the Witwatersrand, 1 Jan Smuts Avenue, Johannesburg, 2050, South Africa

^biThemba LABS, National Research Foundation, PO Box 722, Somerset West, 7129, South Africa

E-mail: anza-tshilidzi.mulaudzi@cern.ch

Abstract. Motivated by the multi-lepton anomalies, a search for narrow resonances with $S \rightarrow \gamma\gamma, Z\gamma$ in association with light jets, b -jets, or missing transverse energy was reported by arXiv:2109.02650. In this paper, we search for scalar resonances in the e^+e^- environment. The final states that are considered are the $Z\gamma \rightarrow jj, l^+l^-$ and $S \rightarrow \gamma\gamma$ and we use machine learning tools to determine the final state with the most significance. A classification model is developed in order to distinguish between the signal and background processes through the use of a Deep Neural Network (DNN) which is constructed using a dataset that consists of the energy, the pseudo-rapidity and azimuthal angle for each of the particles in each final state. The parameters of the DNN are tuned using a hyperparameter optimisation algorithm so that the convergence of the receiver operating characteristic (ROC) curve is achieved.

1. Introduction

The discovery of the Higgs boson [1, 2, 3] at the Large Hadron Collider (LHC), through the ATLAS [4] and CMS [5] experiments, has broadened the field of particle physics. Based on measurements at a mass of 125 GeV for the Higgs, it was found that it is consistent with Standard Model (SM) predictions. This allows us to take into consideration the existence of additional or Higgs-like scalar bosons, but taking into consideration that the mixing with the SM must be adequately small. The multi-lepton anomaly final states at the LHC are observed in refs [6, 7]. They are studied in a two-Higgs doublet model with an additional singlet scalar (2HDM+S), where the masses of the CP -even scalars h, S, H are taken around 125, 150 and 270 GeV, respectively. The presumed dominant decays were $H \rightarrow Sh, SS$. This is encouragement for us to search for scalar resonances concerning $S \rightarrow \gamma\gamma, Z\gamma$ in association with missing transverse energy, light- and b -jets. The coupling information between the scalar S and vector boson pairs is established through the observed decays of S via $WW, ZZ, Z\gamma$ or $\gamma\gamma$ channels.

In Ref [8], an alternative lepton production mechanism are discussed. The scalar S may decay as $S \rightarrow NN$ where N contains the quantum numbers of the right-handed neutrinos. In this configuration, the 2HDM+S can be extended with right-handed neutrinos and this is used to further explain the anomalous muon $g - 2$ measurement through the chiral enhancement as discussed in Refs. [9, 10]. Keeping this in mind, we can review a diegesis where the mixing of the scalar with SM is insignificantly small. The couplings of S to the electroweak gauge

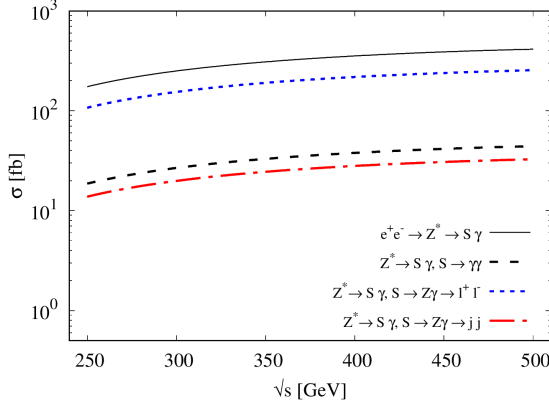


Figure 1: The cross-sections for the production of the singlet scalar of a mass $m_S = 151.5\text{GeV}$ as a function of the centre of mass energy \sqrt{s} in the e^+e^- environment. The black solid line represents the production of S through an off-shell Z^* gauge boson. The dashed blue, black and red lines represent the cross-sections for the S decays where $S \rightarrow \gamma\gamma$ and $S \rightarrow Z\gamma, Z \rightarrow jj, l^+l^-$.

bosons are loop induced and this opens up a pathway to the production of S at future e^+e^- colliders. Subsequently, it allows an opportunity to study the properties of S in final states that are strenuous to isolate in pp collisions. In Figure 1, we the cross-sections of the $S\gamma$ production mechanism. In this proceedings, we aim to show that the cross-section of the singlet scalar is large enough to be detected in future e^+e^- colliders.

2. Model

The electroweak quantum number of S dictates the coupling of S with the electroweak gauge bosons $WW, ZZ, Z\gamma, \gamma\gamma$. The leading order SV_1V_2 couplings originate from the following two five-dimensional operators [11]:

$$\mathcal{L}_{D5} = \kappa_2 \frac{S}{4m_S} W_{\mu\nu}^a W^{a\mu\nu} + \kappa_1 \frac{S}{4m_S} B_{\mu\nu} B^{\mu\nu}, \quad (1)$$

where $\kappa_{1,2}$ are the coupling strengths. In terms of mass eigenstates

$$W^\pm = \frac{1}{\sqrt{2}}(W^1 \mp iW^2), \quad (2)$$

and

$$\begin{pmatrix} W^3 \\ B \end{pmatrix} = \begin{pmatrix} c_w & s_w \\ -s_w & c_w \end{pmatrix} \begin{pmatrix} Z \\ A \end{pmatrix}, \quad (3)$$

these operators can be written as,

$$\begin{aligned} \mathcal{L} = & \kappa_2 \frac{S}{2m_S} W_{\mu\nu}^+ W^{-\mu\nu} + (\kappa_2 c_w^2 + \kappa_1 s_w^2) \frac{S}{4m_S} Z_{\mu\nu} Z^{\mu\nu} \\ & + 2c_w s_w \frac{S}{4m_S} (\kappa_2 - \kappa_1) Z_{\mu\nu} F^{\mu\nu} + (\kappa_2 s_w^2 + \kappa_1 c_w^2) \frac{S}{4m_S} F_{\mu\nu} F^{\mu\nu}. \end{aligned} \quad (4)$$

The cosine and sine of the weak mixing angle are $c_w = g/\sqrt{g^2 + g'^2}$ and $s_w = g'/\sqrt{g^2 + g'^2}$, respectively. From Eq. 4 we can write the couplings as:

$$\Gamma_{SV_1V_2}^{\mu\nu} = \frac{gSV_1V_2}{m_S} (p_{V_1} \cdot p_{V_2} g^{\mu\nu} - p_{V_1}^\nu p_{V_2}^\mu), \quad (5)$$

where $g_{SWW} = \kappa_2$, $g_{SZZ} = (\kappa_2 c_w^2 + \kappa_1 s_w^2)$, $g_{SZ\gamma} = c_w s_w (\kappa_2 - \kappa_1)$, and $g_{S\gamma\gamma} = \kappa_2 s_w^2 + \kappa_1 c_w^2$.

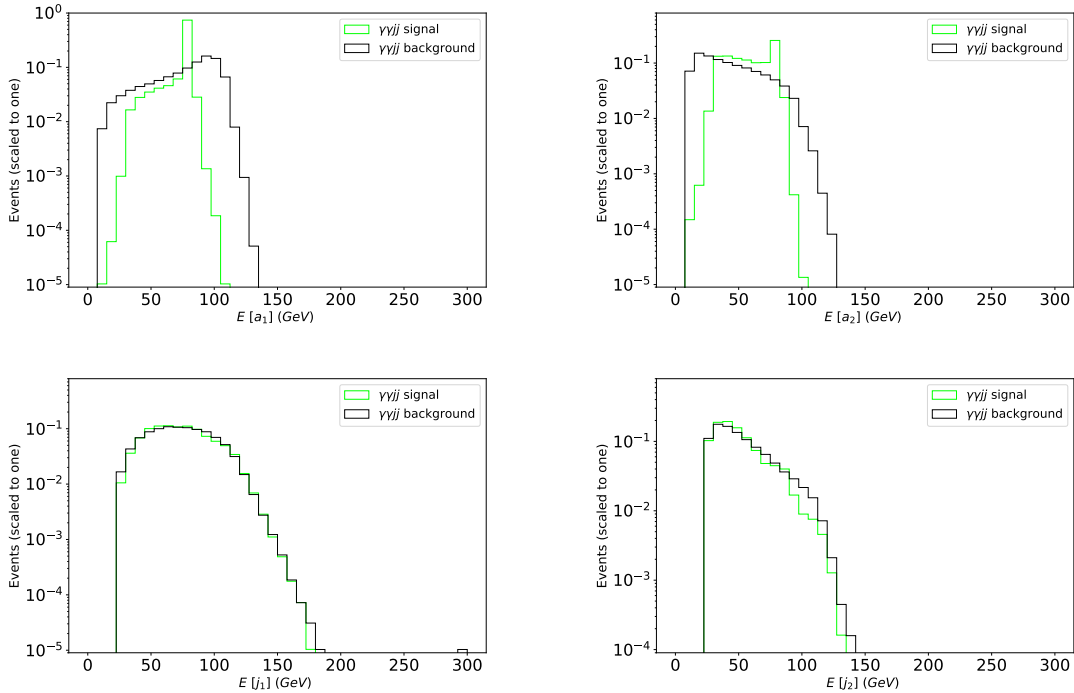


Figure 2: Normalised differential distributions for the energies of the di-jet, di-photon channel: the leading and sub-leading photon (top row) and jet energy (bottom row)

3. Simulation and results

In order to simulate the S production in association with photon through off-shell Z boson in e^+e^- environment, the Lagrangian 4 are implemented in `Feynrules` [12]. The signal and background events are generated using `Madgraph5_aMC@NLO` [13]. Further parton-level events are showered through `Pythia8` [14] to take care of fragmentation and hadronisation. The detector level simulation is performed through `Delphes` [15]. The construction of jets at this level was performed using `Fastjet` [16] which utilizes the anti- k_T jet algorithm with a radius $R = 0.5$ and $p_T > 20$ GeV. In this work, the singlet scalar mass is set to $m_S = 151.5$ GeV.

The signal process is $e^+e^- \rightarrow Z^* \rightarrow S\gamma$, where S further decay to $Z\gamma$, $Z \rightarrow jj, l^+l^-$ and $\gamma\gamma$ final state. The calculations for the production of the SM Higgs boson and other scalars in the context of the Minimal Supersymmetric Model (MSSM) in association with a photon, were done in ref. [17, 18, 19]. They show that this process, although it being rare, it produces a clean final state due to suppressed backgrounds. The presence of an excess in the $Z(\rightarrow l^+l^-)\gamma$ final state in Ref [8] indicates that the branching ratio of $S \rightarrow \gamma\gamma$ is significantly lower than that of $S \rightarrow Z\gamma$. As such, we chose $\kappa_W = -0.014$ and $\kappa_B = 0.028$ ($\kappa_W/\kappa_B = -0.5$) for this study.

3.1. Optimization of the di-jet, di-photon channel using ML technique

In machine learning, various tools and systems are used depending on what task one wants to complete. Based on the data that is obtained from the kinematic distributions (Figures 2, 3), this study will make use of a Sequential Machine Learning method. This method will be implemented through the use of a Deep Neural Network (DNN). A DNN allows us to input and output a series of data sequences. It consists of key features that are termed parameters. The parameters that we use are the number of epochs, neurons, layers, the batch size and the learning rate. The DNN will be used to train our sequential model and test how it efficiently discriminates

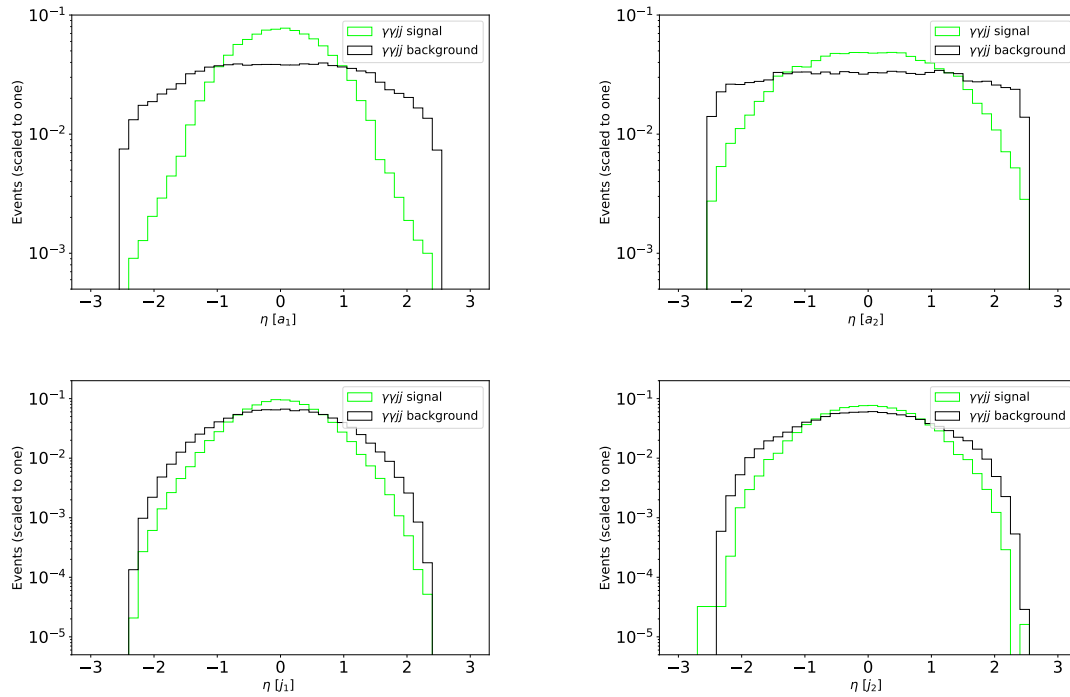


Figure 3: Normalised differential distributions for the pseudorapidities of the di-jet, di-photon channel: the leading and sub-leading photon (top row) and jets (bottom row).

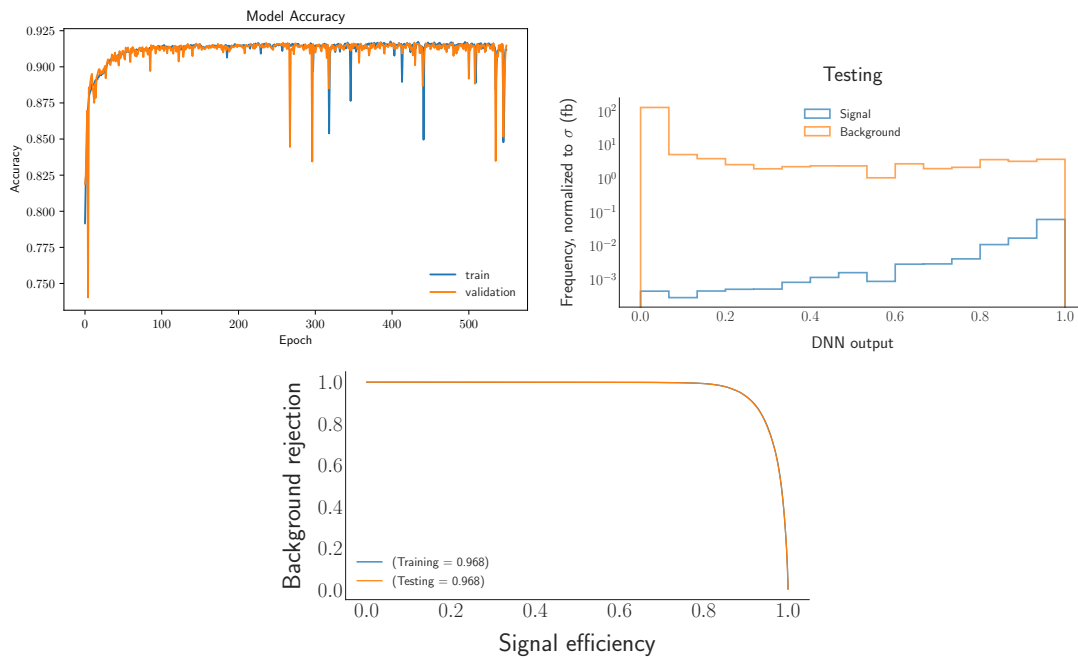


Figure 4: The accuracy (left), DNN output (right) and ROC curve (bottom) of the DNN model, are depicted. An accuracy of 96.8% is achieved with the test sample.

the events from signal and background processes. To ensure that our model converges, we will run a hyperparameter optimisation algorithm to tune the parameters of our model so that they output an optimised model accuracy. This will be achieved once the model accuracy reaches a plateau which subsequently means that the model converges.

In these proceedings, we will show the results for the di-jet, di-photon channel. The input parameters that were used for the DNN dataset were the energy, pseudorapidity and azimuthal angle of the leading and sub-leading jets and photons. Semi-supervised learning is the ML technique that is used. This is to ensure that the model is able to discriminate signal and background events successfully. The number of neurons that the DNN consists were 25, with the layers being 43. The considered batch size was 32 and the number of epochs was 550. The model was set to learn at a rate of 0.0009263. The optimizer of choice was Adam. The resulting accuracy that was achieved was 96.8% as seen in Fig 4. The receiver operating characteristic (ROC) curve depicts the 1:1 ratio of background rejection to the signal efficiency. The DNN outputs for the training and testing samples illustrate a distinct separation of the signal and background events. This is adequate evidence that the scalar can be detected at e^+e^- colliders.

4. Summary and outlook

In this proceedings, we reported a search strategy of a singlet scalar mass $m_S = 151.5$ GeV which couples to SM gauge bosons through dimension five operators in e^+e^- colliders. The associate production of S with a photon via an off-shell Z^* is taken for this study where $S \rightarrow Z\gamma, \gamma\gamma$. Further, we reported an accuracy of 96.8 % for the discrimination of signal and background events for the three photon channel. This was achieved through the use of ML. This work is in progress where we will also take into consideration two other S decay channels, where $S \rightarrow Z\gamma, Z \rightarrow jj, l^+l^-$. We will compare the optimisation of signal over potential backgrounds using conventional and ML techniques and also study the limits on couplings and the potential of future e^+e^- colliders at different centre-of-mass energies to discover the singlet scalar S .

References

- [1] Englert F and Brout R 1964 *Physical review letters* **13** 321
- [2] Guralnik G S, Hagen C R and Kibble T W 1964 *Physical Review Letters* **13** 585
- [3] Higgs P W 1964 *Phys. Lett.* **12** 132–133
- [4] Aad G, Abajyan T, Abbott B, Abdallah J, Khalek S A, Aben R, Abi B, Abolins M, AbouZeid O, Abramowicz H *et al.* 2013 *Physics Letters B* **726** 120–144
- [5] Chatrchyan S, Khachatryan V, Sirunyan A M, Tumasyan A, Adam W, Aguilo E, Bergauer T, Dragicevic M, Erö J, Fabjan C *et al.* 2013 *Physical Review Letters* **110** 081803
- [6] Von Buddenbrock S, Cornell A S, Mohammed A F, Kumar M, Mellado B and Ruan X 2018 *Journal of Physics G: Nuclear and Particle Physics* **45** 115003
- [7] von Buddenbrock S, Chakrabarty N, Cornell A S, Kar D, Kumar M, Mandal T, Mellado B, Mukhopadhyaya B, Reed R G and Ruan X 2016 *The European Physical Journal C* **76** 1–18
- [8] Crivellin A, Fang Y, Fischer O, Kumar A, Kumar M, Malwa E, Mellado B, Rapheeha N, Ruan X and Sha Q 2021 *arXiv preprint arXiv:2109.02650*
- [9] Crivellin A, Hoferichter M and Schmidt-Wellenburg P 2018 *Physical Review D* **98** 113002
- [10] Chun E J and Mondal T 2020 *Journal of High Energy Physics* **2020** 1–20
- [11] Low I and Lykken J 2010 *Journal of High Energy Physics* **2010** 1–20
- [12] Alloul A, Christensen N D, Degrande C, Duhr C and Fuks B 2014 *Computer Physics Communications* **185** 2250–2300
- [13] Allwall J, Frederix R, Frixione S, Hirschi V, Maltoni F, Mattelaer O, Shao H S, Stelzer T, Torrielli P and Zaro M 2014 *Journal of High Energy Physics* **2014** 1–157
- [14] Sjöstrand T, Mrenna S and Skands P 2008 *Computer Physics Communications* **178** 852–867
- [15] De Favereau J, Delaere C, Demin P, Giammanco A, Lemaitre V, Mertens A and Selvaggi M 2014 *Journal of High Energy Physics* **2014** 1–26
- [16] Cacciari M, Salam G P and Soyez G 2012 *The European Physical Journal C* **72** 1–54
- [17] Barroso A, Pulido J and Romao J 1986 *Nuclear Physics B* **267** 509–530
- [18] Abbasabadi A, Bowser-Chao D, Dicus D A and Repko W W 1995 *Physical Review D* **52** 3919

[19] Djouadi A, Driesen V, Hollik W and Rosiek J 1997 *Nuclear Physics B* **491** 68–102